AD-A049 665 OHIO STATE UNIV COLUMBUS ELECTROSCIENCE LAB F/G 9/1
THE EFFECTS OF THE HUMAN BODY ON THE PATTERNS OF THE MANPACK TR--ETC(U)
JUN 77 P MANGIACOTTI, E H NEWMAN DAAG29-76-G-0067
UNCLASSIFIED ESL 4311-4 ARO-13331.4-EL NL

1 OF 1
ADA049665

END
DATE FILMED
3-78
DDC

THE EFFECTS OF THE HUMAN BODY ON THE PATTERNS OF THE MANPACK TRANSCEIVER ANTENNA

Peter Mangiacotti
Edward H. Newman

The Ohio State University

ElectroScience Laboratory

Department of Electrical Engineering
Columbus, Ohio 43212

Technical Report 4311-4
Grant No. DAAG29-76-G-0067
June 1977

Department of the Army
U.S. Army Research Office
Research Triangle Park, North Carolina 27709

NOTICES

When Government drawings, specifications, or other data are used for any purpose other than in connection with a definitely related Government procurement operation, the United States Government thereby incurs no responsibility nor any obligation whatsoever, and the fact that the Government may have formulated, furnished, or in any way supplied the said drawings, specifications, or other data, is not to be regarded by implication or otherwise as in any manner licensing the holder or any other person or corporation, or conveying any rights or permission to manufacture, use, or sell any patented invention that may in any way be related thereto.

The findings in this report are not to be construed as an official Department of the Army position, unless so designated by other authorized documents.

UNCLASSIFIED

SECURITY CLASSIFICATION OF THIS PAGE *(When Data Entered)*

REPORT DOCUMENTATION PAGE	READ INSTRUCTIONS BEFORE COMPLETING FORM
1. REPORT NUMBER	2. GOVT ACCESSION NO. 3. RECIPIENT'S CATALOG NUMBER (9)
4. TITLE *(and Subtitle)* (6) THE EFFECTS OF THE HUMAN BODY ON THE PATTERNS OF THE MANPACK TRANSCEIVER ANTENNA	5. TYPE OF REPORT & PERIOD COVERED Technical Report, (14) 6. PERFORMING ORG. REPORT NUMBER ESL 4311-4
7. AUTHOR(s) (10) Peter Mangiacotti, Edward H. Newman	8. CONTRACT OR GRANT NUMBER(s) (15) Grant NO. DAAG29-76-G-0067
9. PERFORMING ORGANIZATION NAME AND ADDRESS The Ohio State University ElectroScience Laboratory, Department of Electrical Engineering Columbus, Ohio 43212	10. PROGRAM ELEMENT, PROJECT, TASK AREA & WORK UNIT NUMBERS
11. CONTROLLING OFFICE NAME AND ADDRESS Department of the Army U.S. Army Research Office Research Triangle Park, North Carolina 27709 (11)	12. REPORT DATE June 1977 13. NUMBER OF PAGES 20
14. MONITORING AGENCY NAME & ADDRESS *(if different from Controlling Office)* (12) 24 p.	15. SECURITY CLASS. *(of this report)* Unclassified 15a. DECLASSIFICATION DOWNGRADING SCHEDULE

16. DISTRIBUTION STATEMENT *(of this Report)*

Approved for public release; distribution unlimited.

17. DISTRIBUTION STATEMENT *(of the abstract entered in Block 20, if different from Report)*

(18) ARO (19) 13331.4-EL

18. SUPPLEMENTARY NOTES

The material contained in this report is also used as a thesis submitted to the Department of Electrical Engineering, The Ohio State University as partial fulfillment for the degree Master of Science.

19. KEY WORDS *(Continue on reverse side if necessary and identify by block number)*

Antennas
Manpack
Human Body
Dielectric
Moment Method

20. ABSTRACT *(Continue on reverse side if necessary and identify by block number)*

The effects of the human body on the radiation characteristics of the portable manpack transceiver antenna are examined in this report. These effects are demonstrated using numerical techniques employing the method of moments. The human body is modeled as a lossy dielectric and the antenna as a thin-wire radiator. Results presented show the effects of the head, arms, legs, and torso on the far-zone radiation patterns.

DD FORM 1 JAN 73 1473 EDITION OF 1 NOV 65 IS OBSOLETE

UNCLASSIFIED

SECURITY CLASSIFICATION OF THIS PAGE *(When Data Entered)*

TABLE OF CONTENTS

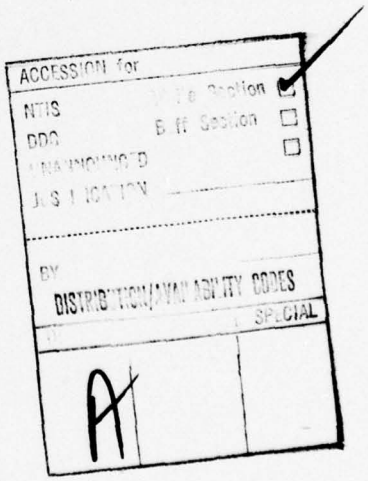

CHAPTER I

INTRODUCTION

A. Background

Portable voice communication transceivers have traditionally been and are still today an important aspect of military communications. The antenna most commonly used on these portable manpack transceivers is the standard monopole or whip. These transceivers usually operate in the low VHF and HF bands, for example, 30 to 76 MHz for the PRC-77 [1]. A 3 foot whip is normally used in this frequency range. Characteristically, the whip antenna approaches a quarter wavelength in height and has high efficiency and an omnidirectional radiation pattern. These are usually desired features for such a communication system. Attempts to substantially reduce the size of the whip usually resulted in a significant loss of antenna efficiency, 10 dB or greater. This loss is a significant factor, considering the limited power available in these portable systems.

B. Purpose

The purpose of this report is to show the effects of the human body on the radiation characteristics of the portable manpack transceiver antenna. The human body is modeled as a lossy dielectric and the antenna is modeled as a thin-wire radiatior. These effects will be demonstrated using numerical techniques which employ the method of moments. The computer program used in this analysis is essentially an extension of work by Tulyathan and Newman [2], which itself is a specific extension of Richmond's thin-wire program [3]. Modifications to Tulyathan and Newman's program were necessary in order to compute the far-fields radiated by the wire antenna in the presence of the dielectric body. The results of these numerical techniques will be compared to previous measurements [1].

C. Outline

A brief outline of the moment method solution of a thin-wire antenna in the presence of a dielectric body is presented in Chapter II. The moment method solution is based on the sinusoidal reaction formulation [4] and is fairly general. The next part of this chapter deals with the computation of the far-fields radiated by the equivalent currents of the wire antenna and the dielectric body.

Numerical calculations based on computer results are presented in Chapter III. Various models of the human body were tested in the computer program. The results of these tests, along with the field pattern characteristics, are given in this section. Finally, Chapter IV summarizes this study and its practical implications.

CHAPTER II

THEORY

The moment method solution using piecewise sinusoidal basis functions for thin-wire antennas in a homogeneous medium is well established by Richmond [4]. This program was modified by Tulyathan [2] to analyze the effects of an arbitrary dielectric or ferrite body in the presence of a thin-wire antenna structure. Antenna current distributions and induced volume polarization currents in the material body were determined by Tulyathan [2]. The above work is extended to permit the computation of far-zone radiation patterns of antennas in the presence of material bodies. To do this, the far-fields radiated by the induced volume polarization currents are added to the far-fields of the wire antenna currents.

The basic theory for a thin-wire antenna in the presence of a dielectric body will now be briefly reviewed. Figure 2-1a shows the geometry of the problem to be considered. The impressed sources $(\underline{J}_i, \underline{M}_i)$, enclosed by volume V_1, radiate the field $(\underline{E}, \underline{H})$ in the presence of two inhomogeneities. The first inhomogeneity is a thin-wire structure in the volume V_w and enclosed by surface S_w. The second inhomogeneity is a dielectric body with consitutive parameters (μ_o, ε) confined to the volume V_2. The ambient medium has parameters (μ_o, ε_o). All sources are time harmonic and the time dependence $e^{j\omega t}$ is suppressed.

The first step in the solution of this problem is to replace the wire and dielectric inhomogeneities by equivalent currents. By the surface equivalence principle of Schelkunoff [5], the wire is replaced by the ambient medium, and the following equivalent surface current densities

$$\underline{J}_s = \hat{n} \times \underline{H} \tag{1}$$

$$\underline{M}_s = \underline{E} \times \hat{n} \tag{2}$$

are introduced on the wire surface S_w, where $\hat{n}$ is the outward normal vector on S_w. Next, the dielectric inhomogeneity is replaced by the ambient medium and equivalent electric volume polarization currents

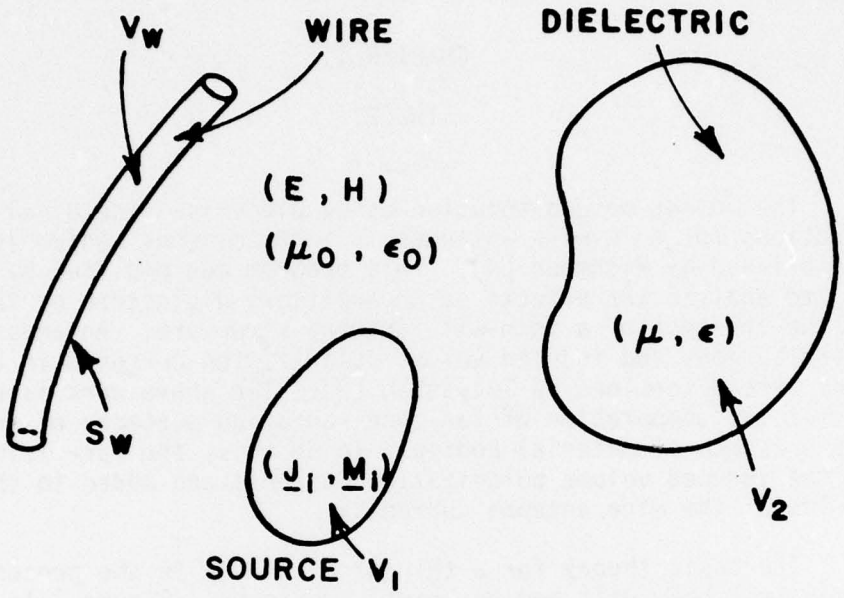

Figure 2-1a--A wire antenna in the presence of a dielectric inhomogeneity.

$$\underline{J} = j\omega(\epsilon-\epsilon_0)\underline{E} \tag{3}$$

which are confined to the volume V_2.

The equivalent problem is shown in Figure 2-1b, where in the homogeneous medium (μ_0,ϵ_0), the sources $(\underline{J}_i,\underline{M}_i)$, $(\underline{J}_s,\underline{M}_s)$ and $\underline{J}$ radiate the fields $(\underline{E},\underline{H})$ exterior to S_W and (0,0) interior to S_W. When radiating in the ambient medium (μ_0,ϵ_0), the sources $(\underline{J}_i,\underline{M}_i)$, $(\underline{J}_s,\underline{M}_s)$ and $\underline{J}$ produce the fields $(\underline{E}_i,\underline{H}_i)$, $(\underline{E}_s,\underline{H}_s)$ and $(\underline{E}^J,\underline{H}^J)$, respectively. In the equivalent problem the currents $(\underline{J}_s,\underline{M}_s)$ and $\underline{J}$ are unknown since the field $(\underline{E},\underline{H})$ is unknown. These currents are determined as follows.

Two coupled integral equations for the unknown currents are now presented. Consider the wire to have a circular cross section defined by the right-handed orthogonal coordinate system with unit vectors $(\hat{n},\hat{\phi},\hat{\ell})$ where $\hat{n}$ is the outward normal vector to S_W, $\hat{\ell}$ is directed along the wire axis and

$$\hat{\phi} = \hat{\ell} \times \hat{n} \quad . \tag{4}$$

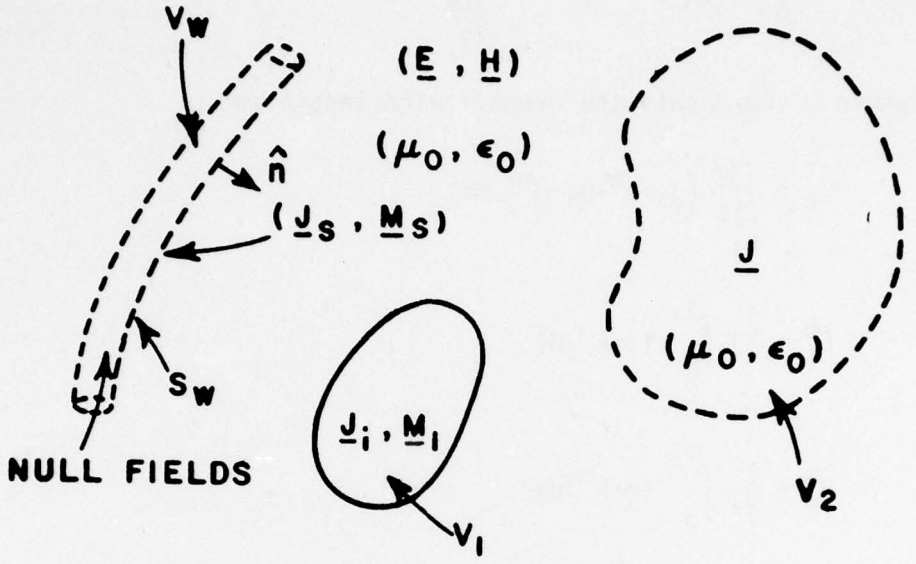

Figure 2-1b--An equivalent problem.

Using the "thin-wire approximation" [4], the surface current $\underline{J}_s$ is related to the total current inside the wire $\underline{I}_{(\ell)}$ by

$$\underline{J}_s(\ell) = \frac{\hat{\ell} I_{(\ell)}}{2\pi a} = \frac{\underline{I}_{(\ell)}}{2\pi a} \quad . \tag{5}$$

Thus, the tangential electric field on the wire surface S_w is

$$\underline{E}_s = Z_s \, \underline{J}_s \tag{6}$$

where Z_s is the surface impedance for exterior excitation. From Equations (2) and (6), the magnetic surface current density is

$$\underline{M}_s = Z_s \underline{J}_s \times \hat{n} = \hat{\phi} \, \frac{Z_s I_{(\ell)}}{2\pi a} \quad . \tag{7}$$

By placing a test source of current density J_m in the interior of the wire volume V_w and employing the reaction integral equation (RIE) [4], we have

$$- \int_0^L I_{(\ell)} \left(E_\ell^m - Z_s H_\phi^m \right) d\ell - \iiint_{V_2} \underline{J} \cdot \underline{E}^m \, dv = V_m \tag{8}$$

where L represents the overall wire length and

$$V_m = \iiint_{V_1} \left(\underline{J}_i \cdot \underline{E}^m - \underline{M}_i \cdot \underline{H}^m \right) dv \tag{9}$$

$$E_\ell^m = \frac{1}{2\pi} \int_0^{2\pi} (\hat{\ell} \cdot \underline{E}^m) d\phi \tag{10}$$

$$H_\phi^m = \frac{1}{2\pi} \int_0^{2\pi} (\hat{\phi} \cdot \underline{H}^m) d\phi \quad . \tag{11}$$

The test source radiates the field $(\underline{E}^m, \underline{H}^m)$ in the ambient medium (μ_o, ε_o).

In the dielectric inhomogeneity, the field $\underline{E}$ is related to the current density $\underline{J}$ by Equation (3). Therefore,

$$\underline{E} = \underline{E_s} + \underline{E^J} + \underline{E_i} = \frac{J}{j\omega(\varepsilon - \varepsilon_o)} \quad \text{in } V_2 \quad . \tag{12}$$

Multiplying Equation (12) by the vector weighting function $\underline{W}_m$ and integrating over the dielectric volume V_2 gives

$$\iiint_{V_2} \left(\underline{E_s} + \underline{E^J} - \frac{\underline{J}}{j\omega(\varepsilon - \varepsilon_o)} \right) \cdot \underline{W}_m \, dv = - \iiint_{V_2} \underline{F_i} \cdot \underline{W_m} \, dv \quad . \tag{13}$$

Thus Equations (8) and (13) are the two coupled integral equations which can be used to solve for the unknown currents $\underline{I}_{(\ell)}$ and $\underline{J}$.

Next we present the moment method solution of these equations. In a rigorous sense, they must be satisfied for arbitrary $\underline{J}_m$ and $\underline{W}_m$. However, in the moment method solution we only enforce them for N distinct $\underline{J}_m$ and M distinct $\underline{W}_m$, which leads to N+M simultaneous linear integral equations. The next step in this solution is to tranform these simultaneous linear integral equations to simultaneous linear algebraic equations. To accomplish this transformation we expand the unknown currents $\underline{I}_{(\ell)}$ and $\underline{J}$ into a finite series as follows:

$$\underline{I}(\ell) = \sum_{n=1}^{N} I_n \, \underline{F_n}(\ell) \tag{14}$$

$$\underline{J} = \sum_{n=N+1}^{N+M} I_n \, \underline{G_n} \tag{15}$$

and substitute these equations into Equations (8) and (13).

In this expansion, $\underline{F_n}(\ell)$ and $\underline{G_n}$ are known as the basis functions and the complex constants I_n are samples of the currents $\underline{I}(\ell)$ and $\underline{J}$. Changing the order of integration and summation we obtain equations of the form

$$\sum_{n=1}^{N} I_n \left\{ - \int_0^L F_n(\ell) \left(E_\ell^m - Z_s H_\phi^m \right) d\ell \right\} + \sum_{n=N+1}^{N+M} I_n \left\{ - \iiint_{V_2} \underline{G_n} \cdot \underline{E}^m dv \right\} = V_m \tag{16}$$

$$\sum_{n=1}^{N} I_n \left\{ \iiint_{V_2} \underline{E_{sn}} \cdot \underline{W_m} \, dV \right\} + \sum_{n=N+1}^{N+M} I_n \left\{ \iiint_{V_2} \left(\underline{E_n^J} - \frac{\underline{G_n}}{j\omega(\epsilon - \epsilon_o)} \right) \cdot \underline{W_m} \, dv \right\}$$

$$= - \iiint_{V_2} \underline{E_i} \cdot \underline{W_m} \, dV \tag{17}$$

where E_{sn} and E_n^J represent the electric fields radiated by $\underline{F_n}$ and $\underline{G_n}$, respectively, in the ambient medium (μ_o, ϵ_o). These equations can be written in compact form as

$$\sum_{n=1}^{N+M} I_n \, Z_{mn} = V_m \, , \quad m = 1, 2, \cdots, N+M \tag{18}$$

or in matrix form as

$$ZI = V$$

where Z is the M x N square impedance matrix, I is the current column containing the unknown expansion coefficients and V is the excitation voltage column.

It is necessary to define specific expansion and weighting functions in order to obtain numerical results from Equations (16) and (17). For the purpose of our analysis we will make use of the following functions. The expansion mode for the wire current is $\underline{F_n}$. For $\underline{F_n}$ we use the piecewise-sinusoidal function used by Richmond [4]. The expansion mode for the electric volume polarization current is $\underline{G_n}$. For $\underline{G_n}$ we use a unit magnitude vector volumetric pulse function. The dielectric volume V_2 is divided into smaller rectangular parallelepipeds or cells. It is necessary to have three orthogonal vector volumetric pulse functions occupying each parallelpiped, since the volume polarization current has arbitrary polarization. Thus, each of the three $\underline{G_n}$ occupying the same cell will have a different polarization, for example, defined by the unit vectors $\hat{x}$, $\hat{y}$ and $\hat{z}$ as shown in Figure 2-2.

For the wire test modes, $\underline{J_m}$, we use the piecewise-sinusoidal function. The choice of piecewise-sinusoidal functions for both the expansion and test modes enable us to use the thin-wire computer program of Richmond [3] to evaluate some elements in the impedance matrix. For the vector weighting function $\underline{W_m}$ we use a delta function located at the center of, and which has the same polarization as, the volumetric pulse expansion function $\underline{G_m}$. If (x_m, y_m, z_m) is the center of $\underline{G_m}$ then

$$\underline{W_m} = \underline{G_m}\, \delta(x-x_m)\delta(y-y_m)\delta(z-z_m) \quad .$$

The result of using this test mode is that Equation (13) is being satisfied at discrete points in volume V_2. This is an application of the point-matching method.

In this analysis we are also interested in the radiation from the dielectric body V_2 and the wire antenna. The effects of the dielectric on the input impedance of the antenna were considered by Tulyathan [2]. Now we will briefly review how to compute the far-field of the composite system. Let $\underline{E}^W$ represent the electric field of the wire current $\underline{I}(\ell)$ and $\underline{E}^D$ represent the electric field of the volume polarization current $\underline{J}$, when radiating in the ambient medium (μ_0, ϵ_0). By superposition, the total field of the composite system is

$$\underline{E} = \underline{E}^W + \underline{E}^D \quad . \tag{19}$$

We can express the electric fields $\underline{E}^W$ and $\underline{E}^D$ in terms of the expansion current modes as follows:

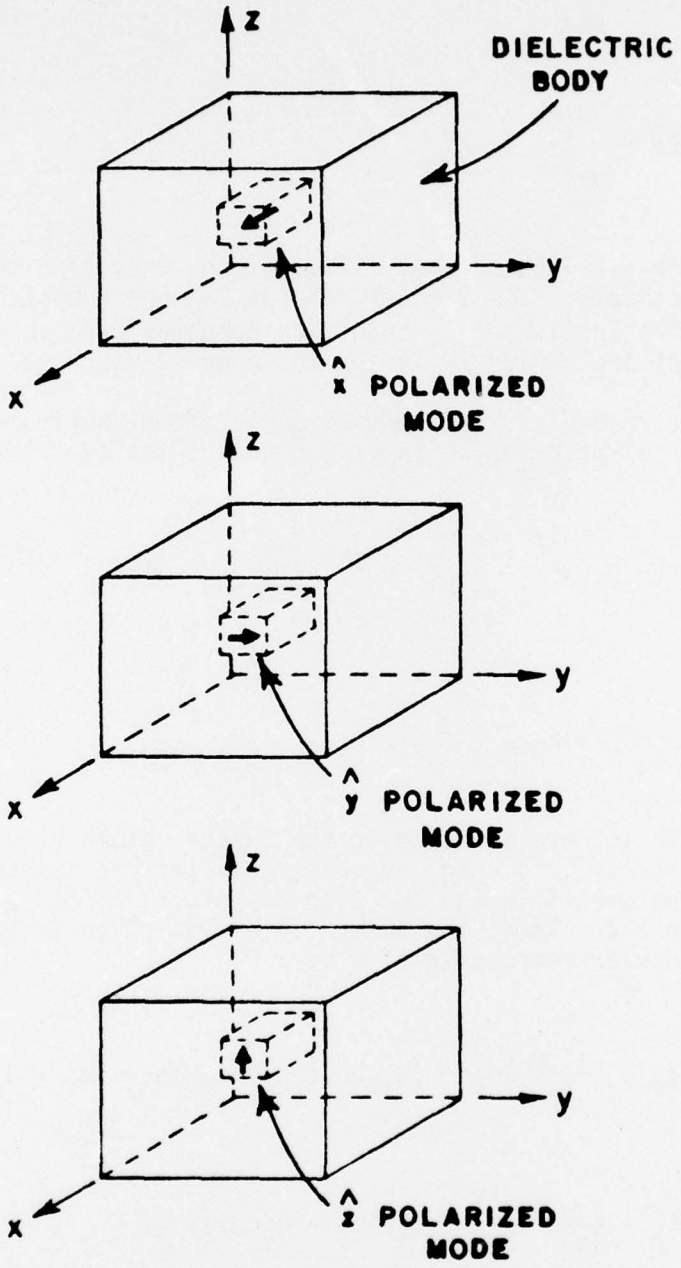

Figure 2-2--A typical volumetric pulse shown with the three polarizations.

$$\underline{E}^W = \sum_{n=1}^{N} I_n \underline{E_{sn}} \tag{20}$$

$$\underline{E}^D = \sum_{n=N+1}^{N+M} I_n \underline{E_n^J} \tag{21}$$

where $\underline{E_{sn}}$ and $\underline{E_n^J}$ are the fields of the expansion modes F_n and G_n, respectively. The electric fields $\underline{E_{sn}}$ are computed using available routines in Richmond's thin-wire computer program [3]. The computation of the fields $\underline{E_n^J}$ in the far-zone is discussed below.

A volume current density $\underline{J}$, as shown in Figure 2-3, radiating in the free space medium (μ_o, ε_o) produces the far field given by

$$\underline{E}(r,\theta,\phi) = -\frac{j\omega\mu_o}{4\pi r} e^{-jkr} \iiint_{V'} \underline{J}(x',y',z') e^{jkg} dV' \tag{22}$$

where

$$g = x'\sin\theta\cos\phi + y'\sin\theta\sin\phi + z'\cos\theta$$

and the integration is over the source volume V' described by coordinates (x',y',z'). In our case, the electric current density $\underline{J}$ is a unit volumetric pulse function of polarizations $\hat{x}$, $\hat{y}$ or $\hat{z}$, as shown in Figure 2-2. Thus, the distant field is given in terms of the constant rectangular components of $\underline{J}$ by

$$E_\theta = -\frac{j\omega\mu_o}{4\pi} \frac{e^{-jkr}}{r} (J_x\cos\theta\cos\phi + J_y\cos\theta\sin\phi - J_z\sin\theta)\, Q \tag{23}$$

$$E_\phi = \frac{j\omega\mu}{4\pi} \frac{e^{-jkr}}{r} (J_x\sin\phi - J_y\cos\phi)\, Q \tag{24}$$

where

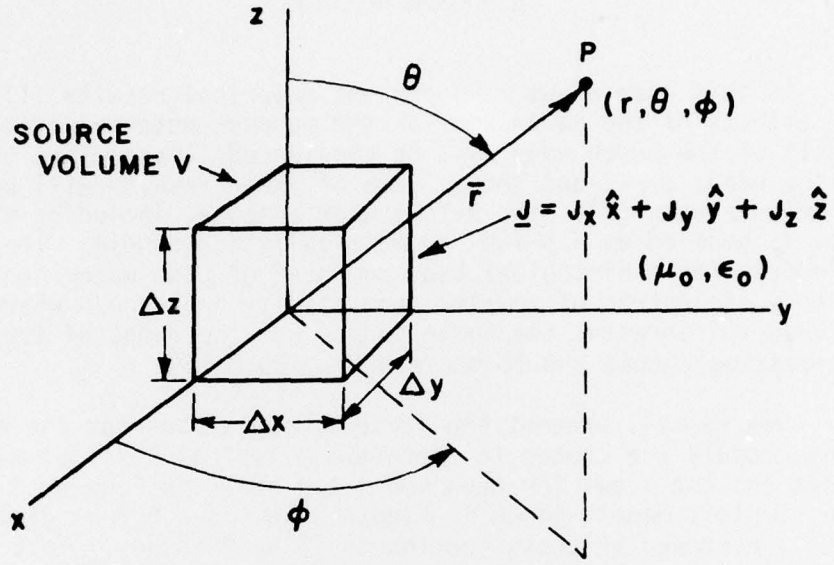

Figure 2-3--A volume current density $\underline{J}$ radiating in free space.

$$Q = \frac{j}{k^3 \sin^2\theta \cos\phi \sin\phi \cos\theta} \left[\left(e^{jk\sin\theta\cos\phi\Delta X} - 1\right)\right.$$

$$\left.\left(e^{jk\sin\theta\sin\phi\Delta Y} - 1\right)\left(e^{jk\cos\theta\Delta Z} - 1\right)\right] \qquad (25)$$

and ΔX, ΔY, ΔZ are the dimensions of the constant current cell. Equations (23) and (24) are thus used to compute the far-zone field associated with each expansion current mode $\underline{G}_n$. As an example of the computation of these fields, consider an expansion mode with $\hat{y}$ polarized current, then $J_x = J_y = 0$. Equations (23) and (24) show that the electric field of this current density has both E_θ and E_ϕ components. Three computations, associated with the $\hat{x}$, $\hat{y}$, and $\hat{z}$ polarizations, are thus required for each cell.

CHAPTER III

NUMERICAL RESULTS

In this chapter we will present numerical results illustrating the effects of the human body on the manpack antenna patterns. Various models of the human body will be considered illustrating the effects of the head, arms, and legs. Some of these results will be compared to measurements [1]. The 3-foot whip antenna, including the manpac set, is modeled as a 6-foot symmetrically fed dipole. The human body is modeled as a biological body composed of high-water-content tissue. A lossy dielectric of complex permittivity $\hat{\varepsilon}=\varepsilon'-j\,\sigma/\omega$ where, $\varepsilon'=\varepsilon_0\varepsilon_r$ is used to represent the human body. For the range of frequencies of interest we choose $\sigma=0.75$ mho/m and $\varepsilon_r=89.0$ [6].

Now we will present the various models used for the human body. These models are chosen to represent a typical six foot man. The front and top views for each model are shown in Figures 3-1(a-h). The simplest model, shown in Figure 3-1a, is a 6 foot dielectric block with a rectangular cross-section of 18 by 9 inches. This model is the crudest representation of the human body. In the next representation a one foot section from the head region of the 6 foot block is removed. Thus, the body is modeled without a head as a 5 foot dielectric block, as shown in Figure 3-1b. In the next level of approximation, the head is modeled using a small dielectric block. This model is shown in Figure 3-1c. In the next model, Figure 3-1d, we attempt to show the effects of the arms and legs. This is done by representing the leg region of the body with a narrower dielectric block and the torso, including the arms, with a wider block. As our best representation of the human body we show the different positions of the arms that may be assumed by the manpac operator. The left arm is at the operator's side in Figure 3-1e, pointing straight ahead in Figure 3-1f, pointing left in Figure 3-1g, and pointing straight up in Figure 3-1h. In these models, the left arm is modeled as a 2 foot long dielectric block, 3 by 4-1/2 inches. The operator's right arm usually assumes a folded position while the manpac transceiver is being operated. We represent this by modeling the right arm as a one foot long block with twice the thickness of the left arm, i.e., 3 by 9 inches. Thus, a total of four dielectric blocks are used in the models of Figures 3-1 (e-h), one each for the arms, head and body.

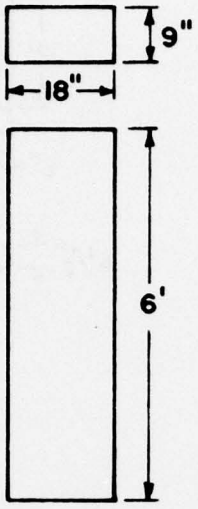

(a) MODEL A - 6 FOOT BLOCK

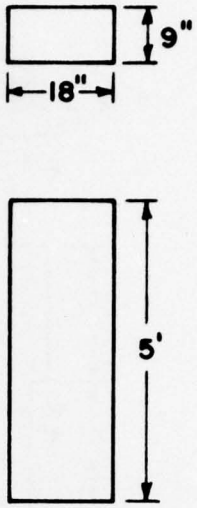

(b) MODEL B - 5 FOOT BLOCK

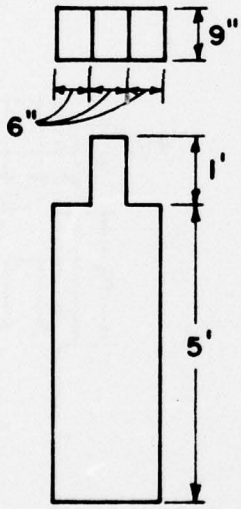

(c) MODEL C - REPRESENTION OF HEAD

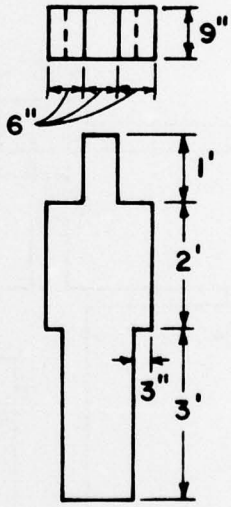

(d) MODEL D - REPRESENTATION OF ARMS AND LEGS

Figure 3-1(a-d)--Dielectric models of human body (top and front views).

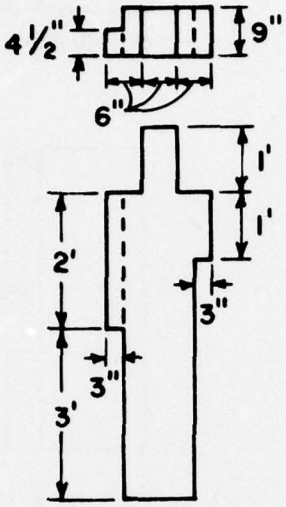

(e) MODEL E – LEFT ARM AT SIDE

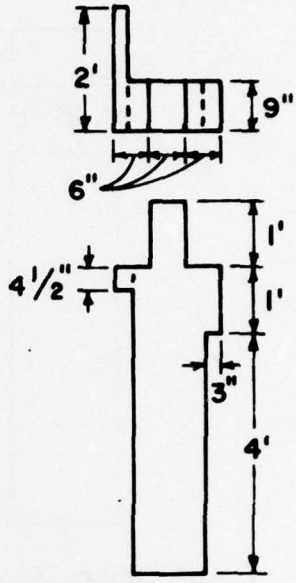

(f) MODEL F – LEFT ARM STRAIGHT AHEAD

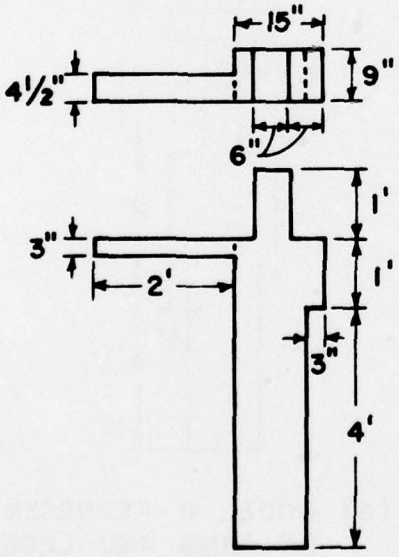

(g) MODEL G – LEFT ARM POINTING LEFT

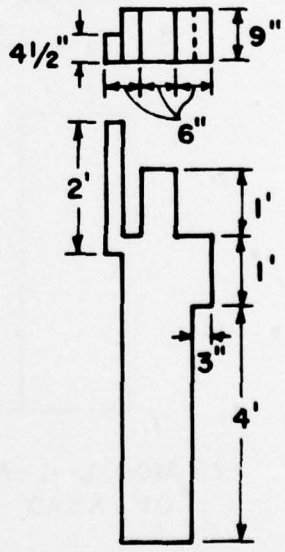

(h) MODEL H – LEFT ARM POINTING UP

Figure 3-1(e-h)-- Dielectric models of human body (top and front views).

A. Pattern Description

The radiation pattern of an ideal dipole antenna in the azimuthal plane is omnidirectional. Thus in the absence of the operator, the manpack whip antenna has essentially the same omnidirectional pattern. In the presence of the human body, the radiation pattern of the whip antenna is perturbed. The geometry and coordinate system for this problem are shown in Figure 3-2.

This figure shows the relative location of the dipole antenna and the dielectric models, using the simple model C of Figure 3-1b. The dipole antenna is located on the z-axis. It is positioned so as to best represent the actual location of the manpack whip antenna with respect to the human operator. The feed point of the whip antenna on the manpac set is essentially at the shoulder level of the operator's right side. Therefore, the feed point of the dipole antenna is located at the 5 foot level for each of the models of Figure 3-1. The most noticable effect on the ideal pattern is that the radiation intensity in the forward direction, through-the-body, is greater than the radiation in the backward direction. Thus, the typical azimuth pattern is a very broad pattern with, beam maximum near $\phi=0°$, a minimum near $\phi=180°$, and no sidelobes. Such broad patterns can be essentially described by the front-to-back ratio.

Now we will present the ratio of the radiation intensity in the forward direction, $\theta=0°$, to the backward direction, $\theta=180°$. These numerical results were calculated using a computer program based on the techniques of the previous chapter [2]. Table 3-1 lists the front-to-back ratios (FTBR) of the radiation pattern, associated with each model of Figure 3-1, and at a frequency of 50 MHz.

TABLE 3-1

Model	Number of Dielectric Blocks	FTBR (dB)	Beam Maximum
A	1	4.91	20°
B	1	1.08	10°
C	2	2.54	20°
D	3	1.60	10°
E	4	2.39	30°
F	4	2.81	30°
G	4	2.10	20°
H	4	-0.19	180°

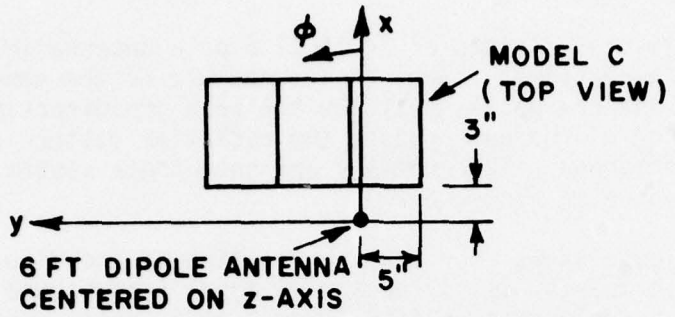

(a) AZIMUTH PLANE

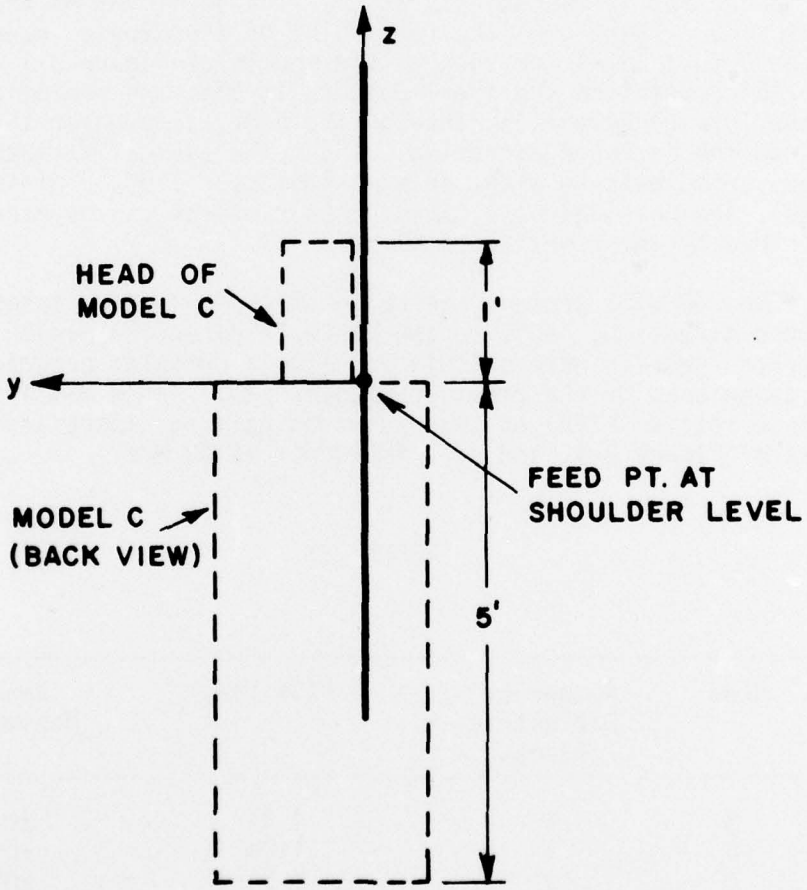

(b) yz PLANE

Figure 3-2--Geometry and coordinate system.

The approximate beam maximum for each model, to the nearest 10°, is also given. Since the dielectric body is not symmetrical about the dipole antenna, the beam maximum is slightly skewed from ϕ=0°. However, this effect is not important since these patterns are very broad in this plane.

Since the manpac transceiver may operate at various frequencies, it would be helpful to examine the effects of frequency on the radiation pattern. Model C, of Figure 3-1c, was used in the computer program to examine these effects. Table 3-2 lists the computed front-to-back ratio and the beam maximum at 30, 40, 50, 60 and 75 MHz. Also listed in this table, for comparison, are the front-to-back ratios obtained from previous measurements [1]. Figure 3-3 shows the computed azimuth patterns at 40 ahd 60 MHz.

TABLE 3-2

Frequency (MHz)	Computed FTBR (dB)	Measurement FTBR (dB)	Beam Maximum
30	0.15	0.5	0°
40	0.74	1.0	0°
50	2.54	2.5	20°
60	8.26	5.5	20°
75	4.64	4.0	20°

Note, that the results of Table 3-2 show a significant increase in the front-to-back ratio at about 60 MHz. Thus, the resonance frequency of a 6 foot man is the vinicity of 60 MHz.

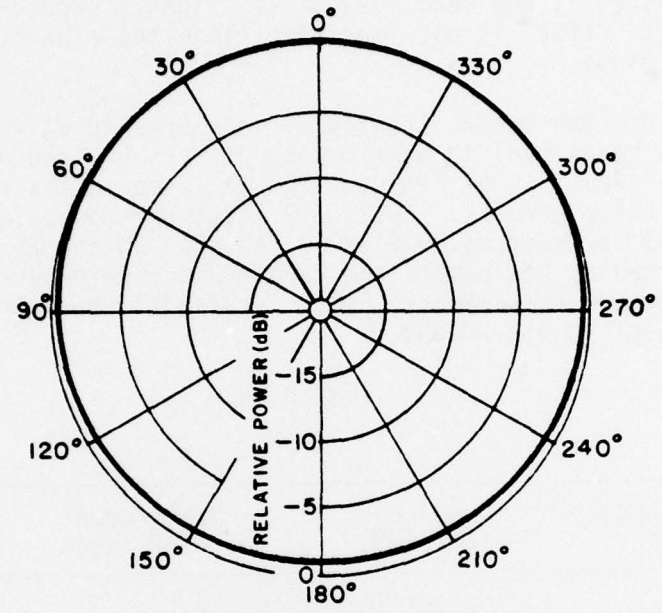

(a) 40 MHz

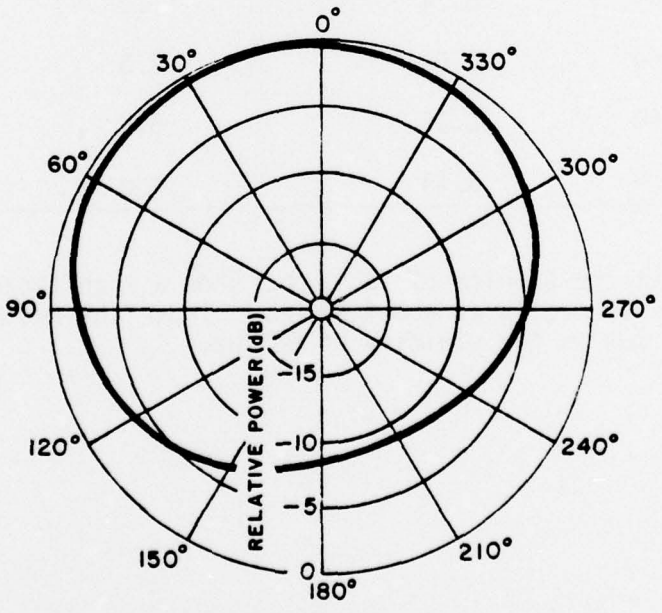

(b) 60 MHz

Figure 3-3--Azimuth plane patterns.

CHAPTER IV

SUMMARY

The purpose of this study has been to show the effects of the human body on the radiation characteristics of the manpack transceiver which uses the monopole whip antenna. The moment method solution for thin-wire antennas in the presence of a dielectric inhomogeneity is presented. This technique is sufficiently general to treat thin-wire antennas or scatterers in the presence of inhomogeneous and lossy dielectric bodies. Computation of the far-zone fields of the composite wire and dielectric body are presented.

Various models of the human body were considered illustrating the effects of the head, arms, legs, and torso. Front-to-back ratios presented indicate that, at most frequencies, the manpac transceiver antenna radiates on the order of one-third more power directly through the human body than in the backward direction. However, when the body length is on the order of one-half wavelength, the front-to-back ratio can be substantially larger.

REFERENCES

1. Bohley, P., R.J. Davis and C.H. Walter, "Man-Pack Loop Antenna System," Report 3824-2, December 1974, The Ohio State University ElectroScience Laboratory, Department of Electrical Engineering; prepared under Contract N00123-74-C-0645 for Naval Regional Procurement Office. (AD/A 006 278)

2. Newman, E. and P. Tulyathan, "Analysis of the Wire Antennas in the Presence of a Dielectric and/or Ferrite Inhomogeneity," Report 4311-2, September 1976, The Ohio State University ElectroScience Laboratory, Department of Electrical Engineering; prepared under Grant DAAG29-76-C-0067 for Department of the Army, Research Triangle Park, N.C. 27709.

3. Richmond, J.H., "Computer Program for Thin-Wire Structures in a Homogeneous Conducting Medium," Report 2902-12, August 1973, The Ohio State University ElectroScience Laboratory, Department of Electrical Engineering; prepared under Grant NGL 36-008-138 for National Aeronautics and Space Administration. (NASA-CR-2399)

4. Richmond, J.H., "Radiation and Scattering by Thin-Wire Structures in the Complex Frequency Domain," Report 2902-10, July 1973, The Ohio State University ElectroScience Laboratory, Department of Electrical Engineering; prepared under Grant NGL 36-008-138 for National Aeronautics and Space Administration.

5. Schelkunoff, S.A., "On Diffraction and Radiation of Electromagnetic Waves," Physical Review, Vol. 56, 15 August 1939, pp. 308-316.

6. Nyquist, Dennis P., Kun-Mu Chen and Bhag S. Guru, "Coupling Between Small Thin-Wire Antennas and a Biological Body," Michigan State University, Department of Electrical Engineering and Systems Science, p. 5.